JOC The Journal of Organic Chemistry

Article

pubs.acs.org/joc

The Nitrogenous Hamigerans: Unusual Amino Acid-Derivatized Aromatic Diterpenoid Metabolites from the New Zealand Marine Sponge *Hamigera tarangaensis*

Jonathan D. Dattelbaum,[†] A. Jonathan Singh,[‡] Jessica J. Field,[‡] John H. Miller,[‡] and Peter T. Northcote*[,‡]

[†]Department of Chemistry, University of Richmond, Richmond, Virginia 23173, United States

[‡]Centre for Biodiscovery, Victoria University of Wellington, Wellington, New Zealand

Supporting Information

ABSTRACT: The NMR-directed isolation and structure elucidation of nine new nitrogenous hamigeran diterpenoids from the New Zealand marine sponge *Hamigera tarangaensis* are described. Featured in this set are the oxazole-containing hamigeran M (**4**) and eight compounds (**5a**−**6a** and **7a**−**8c**) related to the constitutional structure of hamigeran D (**1**). Moderate cytotoxicity in the low-micromolar range against the HL-60 promyeloid leukemic cell line is reported for seven of the new compounds. The structural nature of these compounds suggests that their adducts are derived from an amino acid source and has allowed for revision of the configuration about C-18 of the archetypal compound, hamigeran D, from **1a** to **1b**. The existence of three constitutionally identical forms of hamigeran Q (**8a**−**8c**) requires the involvement of an *allo*-isoleucine stereoisomer and suggests the intriguing possibility of partial prokaryotic biogenesis of these unusual secondary metabolites.

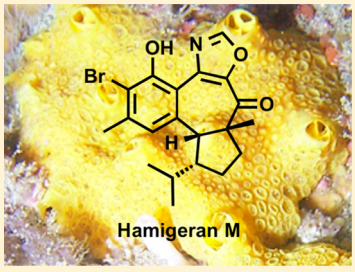

INTRODUCTION

The hamigerans[1,2] are structurally diverse compounds isolated from the New Zealand marine sponge *Hamigera tarangaensis* (Bergquist and Fromont, 1988) that feature a polysubstituted aromatic ring and are adorned with various levels of functionalization about an internal six- or seven-membered B ring. Structures within this series have been the subject of synthetic endeavors because of their molecular complexity and reported biological activities.[3−14] However, of all the hamigeran congeners originally reported by Cambie and co-workers,[1] the structures of hamigeran D (**1a**) and its decomposition product **2a** are perhaps the most intriguing because of the presence of nitrogen in the form of iminoacetal/aminal and amide moieties, respectively. The inclusion of a nitrogen-bearing C_2 unit within the tetracyclic framework was not discussed in any great detail, which is surprising given its deviation from the other reported structures.

We recently reported the NMR-guided isolation of several new hamigeran structures and ascribed their biogenesis to a diterpenoid origin.[2] Among the compounds described, hamigeran G (**3**) was shown to selectively inhibit growth in wild-type and gene-deleted knockout yeast (*Saccharomyces cerevisiae*). Our continued structure-directed investigation of this sponge has led to the isolation of nine nitrogenous hamigeran congeners (**4**, **5a**−**6a**, and **7a**−**8c**; Figure 1) that give perspective on the origin of the nitrogenous adducts. Herein we describe the structure elucidation of these compounds, including hamigeran M (**4**), a new nitrogenous hamigeran containing a 4,5-disubstituted oxazole moiety. This particular structure extends the small number of oxazole-containing terpenoids isolated from the marine environment. Additionally, the first reisolation of hamigeran D since its original description and its structural reassignment from **1a** to **1b** are presented.

RESULTS AND DISCUSSION

Extraction and Isolation. Samples of *H. tarangaensis* collected from Cavalli Island, New Zealand, were subjected to the same extraction and fractionation (PSDVB, LH20) protocols as previously described.[2] Fractions derived from LH20 size-exclusion chromatography were pooled into hamigeran-enriched categories, one of which comprised "classic" hamigeran NMR signatures (e.g., observable phenolic hydroxyl protons) while another contained additional evidence of functionality previously not encountered in this family of compounds. Final purification of this latter fraction utilizing reversed-phase HPLC afforded the reisolation of hamigeran D and nine additional nitrogenous congeners named hamigeran M (**4**), hamigerans N−Q (**5a**, **6a**, **7a**, **8a**, respectively), 19-*epi*-hamigeran Q (**8b**), and 18-*epi*-hamigerans N, P, and Q (**5b**, **7b**, and **8c**, respectively).

Structure Elucidation. The molecular formula of hamigeran M (**4**) was identified through positive-ion HR-ESI-MS analysis ($[M + Na]^+$, m/z 426.0689, Δ = +2.0 ppm) as $C_{20}H_{22}NO_3Br$, for which 10 degrees of unsaturation are required. Eleven of the 20 carbons required by the molecular formula were identified as protonated centers in a multiplicity-edited HSQC experiment: four methyls (δ_C 23.8, 23.5, 23.4, and 21.9), two methylenes (δ_C 37.8 and 28.7), and five

Received: October 15, 2014
Published: November 25, 2014

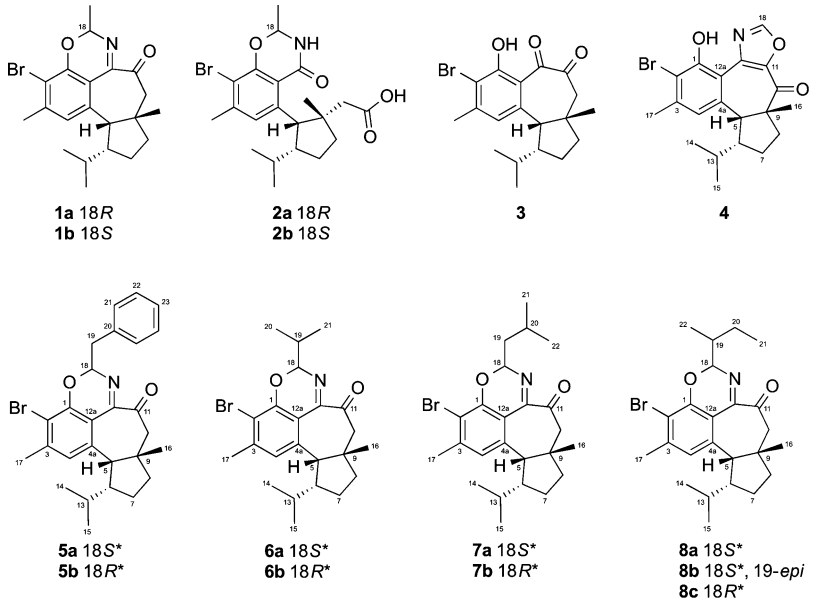

Figure 1. Nitrogenous hamigerans.

Table 1. ^{13}C (150 MHz) and ^{1}H (600 MHz) NMR Data for Hamigeran M (4) in $CDCl_3$

	^{13}C			^{1}H				
position	δ_C	mult.	$^{1}J_{CH}$ (Hz)[a]	δ_H	mult. (*J*, Hz)	COSY	HMBC	NOESY
1	155.2	C						
1-OH				12.57	s		1, 2, 12a	18
2	113.6	C						
3	142.7	C						
4	127.2	CH	160	6.80	s	5, 17	1(w),[b] 2, 3(w), 4a(w), 5, 12,[c] 12a, 17	5, 6, 15, 17
4a	138.6	C						
5	59.9	CH	124	3.28	d (10.3)	4, 6	4, 4a, 6, 8(w), 9, 10, 12a, 13, 16	4, 6, 7a,[d] 8a,[d] 16
6	51.6	CH	121	2.12	m	5, 7a, 7b, 8a, 8b, 13	5, 7, 9, 13, 14, 15	4, 5, 7a,[d] 7b, 8a,[d] 13, 14, 15
7	28.7	CH_2	127	1.35	m	6, 7b, 8a, 8b	6, 8, 13	5, 6, 7b, 8b, 13, 14, 16
			128	1.93	m	6, 7a, 8a, 8b	5, 6, 8, 9, 10(w), 13	6, 7a,[d] 8a,[d] 8b, 14
8	37.8	CH_2	122	1.35	m	6, 7a, 7b, 8b	7, 9, 10, 11,[c] 16	5, 6, 7b, 8b, 13, 14, 16
			136	2.79	m	6, 7a, 7b, 8a	4a, 5, 6, 7, 9, 10	7a,[d] 7b, 8a,[d] 16
9	55.3	C						
10	191.6	C						
11	143.4	C						
12	143.1	C						
12a	111.6	C						
13	31.9	CH	125	1.03	m	6, 14, 15	6, 14, 15	6, 7a,[d] 8a,[d] 14, 15
14	21.9	CH_3	125	0.56	d (6.5)	13, 15	6, 13, 15	6, 7a,[d] 7b, 8a,[d] 13, 15
15	23.4	CH_3	125	0.24	d (6.2)	13, 14	6, 13, 14	4, 6, 13, 14
16	23.5	CH_3	128	1.17	s		5, 8, 9, 10	5, 7a,[d] 8a,[d] 8b
17	23.8	CH_3	129	2.44	s	4	1(w), 2, 3, 4, 12a(w)	4
18	151.5	CH	234	8.22	s		11,[c] 12[c]	1-OH

[a]Obtained from a fully coupled HSQC experiment. [b]Weak correlation. [c]Observed in a band-selected HMBC experiment optimized for an F1 bandwidth of δ_C 110−160. [d]Indistinguishable.

methines (δ_C 151.5, 127.2, 59.9, 51.6, and 31.9). The nine nonprotonated centers were separated into three categories: an α,β-unsaturated ketone (δ_C 191.6), seven aromatic/olefinic carbons (δ_C 155.2, 143.4, 143.1, 142.7, 138.6, 113.6, and 111.6) and an sp^3-hybridized quaternary center at δ_C 55.3. Further inspection of the 1D and 2D NMR experimental data (see Table 1) identified hamigeran-like signatures, including a shielded isopropyl unit, an aromatic methyl, and an exchangeable proton at δ_H 12.57, and also revealed the presence of an unusual sp^2-hybridized methine (δ_H 8.22, δ_C 151.5, $^{1}J_{CH}$ = 234 Hz). These features, coupled with the requirement of nitrogen from the molecular formula, suggest the structure of **4** to be quite removed from any of the other hamigeran compounds described to date.

Interpretation of the COSY and HMBC experimental data identified the same tricyclic core associated with the norisohamigerane skeleton, included in which were the shielded ketone residue (C-10, δ_C 191.6) and two sp^2-hybridized

dx.doi.org/10.1021/jo502370b | J. Org. Chem. 2015, 80, 304−312

carbons (δ_C 143.4 and 143.1) at positions C-11 and C-12, respectively. Furthermore, the remaining nitrogen and oxygen required incorporation with the sp^2 methine and the final two double-bond equivalents. The use of a band-selected HMBC experiment proved crucial in the establishment of the final substructure. The increased resolution in F1 (^{13}C) aided in the revelation of long-range correlations from H-4 (δ_H 6.80) to C-12 (δ_C 143.1) and from H-18 (δ_H 8.22) to both C-11 (δ_C 143.4) and C-12 (Figure 2). From this, two possible

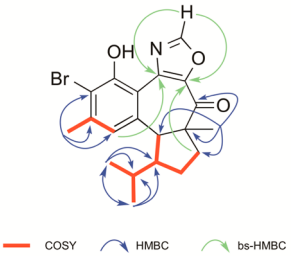

Figure 2. Key 2D NMR correlations used to establish the planar structure of hamigeran M (**4**).

substructures were proposed that were consistent with the observed oxidation state and large $^1J_{CH}$ value of the CH-18 methine: a 1*H*-azirine with a pendant formyl group or a 4,5-disubstituted oxazole. The former structure was entertained but ultimately dismissed because of its noted instability and the lack of precedent in the chemical literature, as evidenced recently by the structural revision of acremolin, a fungus-derived marine natural product.[15−17] The oxazole ring was preferred upon comparison to the synthetic compound 1-[4-(4-fluorophenyl)-1,3-oxazol-5-yl]ethan-1-one prepared by Sisko et al.;[18] the electronic effects due to the substituents in this compound provided excellent agreement with the relevant ^{13}C chemical shifts of hamigeran M (**4**). The relative configuration about the three stereogenic centers of **4** was determined to be identical to known hamigerans through concomitant 2D-NOESY correlations between H-5 (δ_H 3.28, d, 10.3 Hz), H-6, and H_3-16.

Hamigeran N (**5a**) was assigned a molecular formula of $C_{27}H_{30}NO_2Br$ through the interpretation of HR-ESI-MS data ($[M + Na]^+$, m/z 502.1358, Δ = +1.2 ppm). The observation of 25 resonances in the ^{13}C NMR spectrum implied a degree of symmetry in the compound, while the multiplicity-edited HSQC experiment confirmed the attachment of all 30 protons to carbon (see Table 2 and the Supporting Information). Interpretation of COSY and HMBC spectroscopic data provided evidence of the norisohamigerane carbon skeleton and also included resonances attributed to a monoalkyl-substituted benzene unit [δ_C 130.4, δ_H 7.54 (d, 7.0 Hz, 2H); δ_C 128.4, δ_H 7.36 (t, 7.3 Hz, 2H); δ_C 126.9, δ_H 7.28 (t, 7.7 Hz, 1H)] (Figure 3). This subunit group formed part of an isolated spin system that terminated with methine CH-18 (δ_H 5.08, δ_C 90.4), from which HMBC correlations to the phenolic carbon C-1 (δ_C 155.2) and imine C-12 (δ_C 161.1) formed the basis of an aminal center consistent with that observed in the planar structure of hamigeran D (**1**). The relative configuration about CH-5, CH-6, and C-9 for hamigeran N (**5a**), assigned through interpretation of the 2D-NOESY experiment, appears to be consistent with those of all other hamigeran compounds reported to date. A NOE correlation between H-13 and H-18 implies the relative configuration of C-18 to be *S**.

Hamigeran O (**6a**) was assigned a molecular formula of $C_{23}H_{30}NO_2Br$ through the interpretation of HR-ESI-MS data ($[M + Na]^+$, m/z 454.1354, Δ = +0.4 ppm). Analysis of COSY and HMBC spectroscopic data provided evidence of the norisohamigerane carbon skeleton and included a second distinct isopropyl moiety that again terminated with methine CH-18 (δ_H 4.69, δ_C 93.4). 2D NOESY correlation data placed the same relative configuration about the four stereogenic centers in common with hamigeran N (**5a**).

The molecular formula of $C_{24}H_{32}NO_2Br$ for hamigeran P (**7a**) was identified by analysis of HR-ESI-MS data ($[M + Na]^+$, m/z 468.1506, Δ = −0.5 ppm). Inspection of the ^1H and ^{13}C NMR data (see Table 2) showed similar characteristics to hamigeran O (**6a**), including two sets of isopropyl methyls, though their respective molecular formulas differ by the addition of a single CH_2 unit in favor of **7a**. Again, the norisohamigerane skeleton was constructed through standard interpretation of COSY and HMBC data (see Figure 3 and the Supporting Information) and, together with the positional confirmation of C-12 (δ_C 160.9), confined the additional methylene to the nitrogenous side chain. The multiplicity of the aminal methine proton H-18 (δ_H 4.97, dd, J = 7.5, 5.3 Hz) revealed this position to be the most changed through the incorporation of the extra methylene unit and extension of the side chain to form an isobutyl group. In a similar fashion as hamigeran O (**6a**), the observation of through-space correlations between methines H-18 and H-13 in **7a** indicated the retention of relative configuration at these positions.

Compounds **5b** and **7b**, which are isomeric with hamigerans N and P, respectively, were also isolated. Structure elucidation of each compound established the same connectivity as their counterparts, and each compound was found to be epimeric about the C-18 aminal (for NMR data, see Table 3 and the Supporting Information). These two compounds feature the presence of a second solution conformer with a significant downfield shift of H-18 pointing to a change in the chemical environment. For both **5b** and **7b**, there is distinct evidence in the respective 1D and 2D NOESY experiments for dynamic exchange between the two conformers, in the form of either co-irradiation (1D NOESY) or in-phase correlations (2D NOESY). These dynamic effects were also observed in compounds **5a**, **6a**, and **7a** but were attributed to a second conformer present at a much lower level. Spectroscopic evidence exists for a compound consistent with 18-*epi*-hamigeran O (**6b**), which coeluted with hamigeran O (**6a**). However, because of the small sample size, the compound could not be fully purified to unequivocally confirm its structure.

The magnitude of the $^1J_{CH}$ coupling constant for CH-18 in compounds **5a**, **6a**, and **7a**, where the relative configuration is *S**, is on the order of 155 Hz, whereas the corresponding C-18 epimers **5b** and **7b** display couplings of 155 Hz (H-18 upfield) and 175 Hz (H-18 downfield) for their two respective conformers. These observations are consistent with the Perlin effect[19,20] and its associated diagnosis of the configuration about the anomeric center of pyranose sugars, in which the $^1J_{CH}$ value of an axial hydrogen is approximately 10 Hz smaller than the corresponding equatorial hydrogen arrangement. In hamigerans N (**5a**) and P (**7a**), H-18 is pseudoaxial below the plane of the heterocyclic six-membered ring, as indicated by NOE correlations to the isopropyl methine H-13. This assignment is also consistent with the greater magnitude of the vicinal ($^3J_{CH}$) coupling of H-18 to C-1 and C-12 for the

dx.doi.org/10.1021/jo502370b | J. Org. Chem. 2015, 80, 304−312

Table 2. ^{13}C (150 MHz) and ^{1}H (600 MHz) NMR Data for Hamigerans 1b, 5a, 6a, 7a, 8a, and 8b in $CDCl_3$[a]

	1b		5a		6a		7a		8a		8b	
position	δ_C mult.	δ_H mult. (J, Hz)	δ_C mult.	δ_H mult. (J, Hz)	δ_C mult.	δ_H mult. (J, Hz)	δ_C mult.	δ_H mult. (J, Hz)	δ_C mult.	δ_H mult. (J, Hz)	δ_C mult.	δ_H mult. (J, Hz)
1	155.4 C		155.2 C		155.2 C		155.3 C		155.3 C		155.3 C	
2	110.7 C		111.0 C		111.0 C		110.9 C		110.9 C		111.0 C	
3	144.4 C		144.5 C		144.1 C		144.3 C		144.1 C		144.1 C	
4	129.3 CH	6.82 s	129.4 CH	6.80 s	129.2 CH	6.80 s	129.3 CH	6.82 s	129.1 CH	6.80 s	129.1 CH	6.80 s
4a	138.4 C		138.4 C		138.3 C		138.3 C		138.3 C		138.2 C	
5	59.4 CH	3.27 d (10.9)	59.5 CH	3.26 d (10.8)	59.5 CH	3.26 d (10.9)	59.5 CH	3.27 d (11.0)	59.5 CH	3.26 d (10.9)	59.5 CH	3.26 d (10.8)
6	54.0 CH	1.93 m	54.0 CH	1.91 tdd (12.7, 10.8, 6.6)	54.1 CH	1.92 m	54.0 CH	1.93 m	54.1 CH	1.91 m	54.1 CH	1.93 m
7	32.0 CH_2	1.15 qd (13.2, 6.4)	32.0 CH_2	1.13 qd (13.4, 6.3)	32.0 CH_2	1.14 m	32.0 CH_2	1.15 qd (13.3, 6.2)	32.0 CH_2	1.15 m	32.0 CH_2	1.16 m
		1.72 dt (13.6, 6.4)		1.71 dt (13.1, 6.2)		1.70 dt (13.4, 6.5)		1.71 dt (13.3, 6.4)		1.71 dt (13.2, 6.4)		1.71 dt (13.1, 6.4)
8	40.0 CH_2	1.58 dd (13.1, 6.4)	40.0 CH_2	1.59 td (13.0, 6.4)	40.0 CH_2	1.57 m	40.0 CH_2	1.58 m	40.0 C	1.57 m	40.0 C	1.57 m
		2.03 dd (13.2, 6.1)		2.03 dd (13.0, 6.0)		2.03 dd (13.5, 6.2)		2.03 dd (13.1, 6.0)		2.03 dd (13.2, 6.1)		2.03 dd (13.1, 6.0)
9	47.0 C		47.0 C		47.0 C		47.0 C		47.0 C		47.0 C	
10	55.0 CH_2	2.47 d (11.5)	55.1 CH_2	2.47 d (11.6)	55.1 CH_2	2.46 d (11.1)	55.1 CH_2	2.47 d (11.8)	55.1 CH_2	2.45 d (11.5)	55.1 CH_2	2.46 d (11.7)
		2.64 d (11.5)		2.64 d (11.5)		2.65 d (11.4)		2.64 d (11.4)		2.64 d (11.5)		2.64 d (11.7)
11	196.7 C		196.6 C		196.7 C		196.7 C		196.6 C		196.6 C	
12	161.0 C		161.1 C		161.1 C		160.9 C		161.1 C		161.1 C	
12a	118.0 C		118.1 C		118.0 C		118.1 C		118.0 C		117.9 C	
13	29.7 CH	0.85 m	29.6 CH	0.80 m	29.6 CH	0.84 m	29.6 CH	0.85 m	29.6 CH	0.85 m	29.6 CH	0.85 m
14	22.3 CH_3	0.68 d (6.6)	22.3 CH_3	0.66 d (6.5)	22.3 CH_3	0.69 d (6.6)	22.3 CH_3	0.69 d (6.5)	22.3 CH_3	0.68 d (6.7)	22.3 CH_3	0.68 d (6.6)
15	22.5 CH_3	0.38 d (6.1)	22.5 CH_3	0.35 d (6.4)	22.6 CH_3	0.40 d (6.3)	22.6 CH_2	0.41 d (6.2)	22.6 CH_3	0.40 d (6.1)	22.6 CH_3	0.40 d (6.3)
16	32.5 CH_3	1.28 s	32.6 CH_3	1.28 s	32.6 CH_3	1.28 s	32.5 CH_3	1.28 s	32.6 CH_3	1.28 s	32.6 CH_3	1.28 s
17	23.5 CH_3	2.45 s	23.4 CH_3	2.41 s	23.4 CH_3	2.44 s	23.4 CH_3	2.44 s	23.4 CH_3	2.44 s	23.4 CH_3	2.44 s
18	86.7 CH	5.11 q (6.0)	90.4 CH	5.08 dd (9.1, 2.6)	93.4 CH	4.69 d (5.2)	88.6 CH	4.97 dd (7.5, 5.3)	93.0 CH	4.74 d (4.9)	92.4 CH	4.80 d (4.5)
19	21.8 CH_3	1.95 d (6.1)	42.5 CH_2	3.57 dd (14.5, 9.2)	33.3 CH	2.49 m	44.6 CH_2	2.18 m	39.6 CH	2.26 m	39.9 CH	2.28 m
				3.66 dd (14.5, 2.7)								
20			136.9 C		18.2 CH_3	1.25 d (6.8)	24.5 CH	2.19 m	23.7 CH_2	1.41 m	25.3 CH_2	1.52 m
										1.89 m		1.88 m
21			130.5 CH	7.54 d (7.7)	17.0 CH_3	1.19 d (6.8)	22.5 CH_3	1.05 d (6.2)	11.8 CH_3	1.01 t (7.6)	11.8 CH_3	1.03 t (7.4)
22			128.4 CH	7.36 t (7.5)			23.4 CH_3	1.08 d (6.2)	14.7 CH_3	1.22 d (6.9)	13.7 CH_3	1.15 d (6.9)
23			126.9 CH	7.28 tt (7.4, 1.1)								

[a]For full NMR data, see the Supporting Information.

dx.doi.org/10.1021/jo502370b | J. Org. Chem. 2015, 80, 304−312

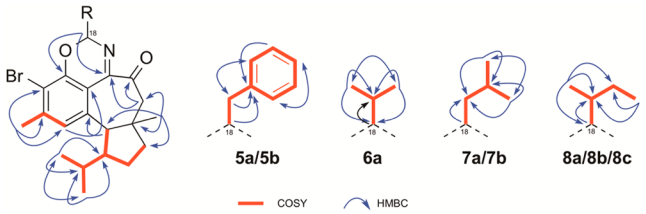

Figure 3. Key COSY and HMBC correlations used to establish the planar structures of compounds **5a**–**6a** and **7a**–**8c**.

pseudoequatorial conformer compared with the pseudoaxial conformer, as observed in the HMBC experiment.[21] In compounds **5b** and **7b**, epimerization about C-18 results in a configuration where the heterocyclic ring undergoes a facile dynamic ring flip. When H-18′ is pseudoaxial above the plane of the ring, both the δ_H and $^1J_{CH}$ values are similar to those of **5a** and **7a**. In the chair-flipped pseudoequatorial arrangement, corresponding increases in both δ_H and $^1J_{CH}$ for CH-18′ are observed. Consistent with this assignment of relative configuration is the observation of weak NOE correlations between the C-19′ methylene and C-13′ methine in both 18-*epi*-hamigerans N (**5b**) and P (**7b**). These observations are summarized in Figure 4.

Compounds **8a**–**c**, each with a molecular formula of $C_{24}H_{32}NO_2Br$ assigned through HR-ESI-MS, are collectively isomeric with hamigeran P (**7a**). The obvious difference between the planar structures **7a** and **8a**–**c** resides in the nitrogenous side chain, in which the change in multiplicity of aminal proton H-18 and the connectivity of methyl centers H_3-21 and H_3-22 led to their respective side chains being established as a *sec*-butyl fragment (Figure 3). For compounds **8a** and **8b**, the conservation of relative configuration within the norisohamigerane skeleton and at CH-18 was confirmed by 2D NOESY correlation data. Thus, the relative configuration of CH-19, while unresolved, implies that compounds **8a** and **8b** must be epimeric at this position and are therefore named as hamigeran Q and 19-*epi*-hamigeran Q, respectively. The third

Table 3. ^{13}C (150 MHz) and ^{1}H (600 MHz) NMR Data for Hamigerans 5b, 7b, and 8c in $CDCl_3$[a]

	5b/5b′ [b]		**7b/7b′** [b]		**8c/8c′** [b]	
position	δ_C mult.	δ_H mult. (*J*, Hz)	δ_C mult.	δ_H mult. (*J*, Hz)	δ_C mult.	δ_H mult. (*J*, Hz)
1	154.7/152.0 C		155.0/152.2 C		154.7/152.4 C	
2	109.6/112.3 C		109.7/112.1 C		109.7/111/6 C	
3	144.4/144/7 C		144.2/144.1 C		143.7/144.0 C	
4	123.0/129.4 CH	6.96 s/6.87 s	122.9/129.1 CH	6.98 s/6.79 s	122.7/129.0 CH	6.97 s/6.79 s
4a	138.4/138.2 C		138.0/138.3 C		138.2/137.7 C	
5	52.94/59.5 CH	2.81 d (4.7)/3.30 d (11.4)	52.9/59.5 CH	2.84 d (4.8)/3.25 d (11.2)	52.8/59.5 CH	2.83 d (4.7)/ 3.25 d (11.1)
6	50.0/53.6 CH	2.16 m/2.03 m	50.0/53.7 CH	2.17 m/1.97 dq (11.1/7.1)	50.0/53.7 CH	2.17 m/1.97 m
7	27.8/31.8 CH_2	1.75 m/1.32 qd (13.3, 6.4)	27.8/31.7 CH_2	1.77 m/1.24 m	27.8/31.7 CH_2	1.77 m/1.23 m
		2.16 m/1.77 m		2.17 m/1.72 m		2.17 m/1.73 m
8	37.1/40.7 CH_2	1.65 m/1.63 m	37.1/40.6 CH_2	1.66 m/1.58 m	37.1/40.6 CH_2	1.67 m/1.59 m
		1.71 m/2.07 m		1.71 m/2.03 dd (13.0, 6.2)		1.71 m/ 2.05 dd (13.5, 6.4)
9	45.1/47.5 C		45.2/47.3 C		45.2/47.2 C	
10	52.86/54.8 CH_2	2.44 m/2.52 d (11.5)	52.8/54.8 CH_2	2.42 m/2.49 d (11.4)	52.9/54.8 CH_2	2.43 m/2.50 d (11.6)
		2.48 m/2.66 d (11.6)		2.49 d (11.4)/2.65 d (11.7)		2.50 d (10.9)/ 2.66 d (11.6)
11	196.0/197.3 C		196.2/197.3 C		196.0/196.7 C	
12	163.1/158.7 C		163.0/158.3 C		163.2/158.1 C	
12a	118.3/116.7 C		118.4/116.9 C		118.1/117.2 C	
13	29.4/30.1 CH	2.04 m/1.05 m	29.4/29.7 CH	2.09 m/0.90 m	29.4/29.6 CH	2.10 m/0.87 m
14	22.8/22.4 CH_3	0.97 d (6.4)/0.73 d (6.5)	22.8/22.1 CH_3	0.99 d (6.7)/0.70 d (6.5)	22.8/22.1 CH_3	0.99 d (6.3)/ 0.71 d (6.7)
15	22.17/22.24 CH_3	0.55 d (6.4)/0.40 d (6.3)	22.3/22.4 CH_3	0.61 d (6.3)/0.35 d (6.2)	22.3/22.6 CH_3	0.61 d (6.4)/ 0.37 d (6.2)
16	25.8/32.2 CH_3	1.25 s/1.27 s	25.8/32.3 CH_3	1.25 s/1.25 s	25.8/32.3 CH_3	1.25 s/1.25 s
17	24.2/23.6 CH_3	2.44 s/2.47 s	24.2/23.5 CH_3	2.47 s/2.43 s	24.1/23.5 CH_3	2.46 s/2.43 s
18	90.67/90.74 CH	5.04 dd (8.8, 3.2)/ 6.28 dd (9.4, 3.2)	88.9/88.5 CH	4.96 dd (6.9, 5.7)/ 6.23 dd (8.3, 5.0)	92.6/93.8 CH	4.76 d (4.7)/ 5.83 d (9.2)
19	42.3/35.7 CH_2	3.56 dd (14.5, 8.7)/2.91 dd (14.4,9.5)	44.5/38.4 CH_2	2.18 m/1.61 m	39.7/36.9 CH	2.28 m/1.81 m
		3.65 dd (14.5, 3.4)/ 3.11 dd (14.4, 3.2)				
20	136.8/135.6 C		24.4/24.5 CH	2.19 m/1.88 m	25.1/24.7 CH_2	1.50 m/1.34 m
						1.89 m/1.70 m
21	130.3/129.8 CH	7.49 d (7.5)/7.16 d (7.3)	22.5/22.1 CH_3	1.04 d (6.2)/1.00 d (6.7)	11.8/11.7 CH_3	1.03 t (7.5)/ 0.88 t (7.5)
22	128.4/128.7 CH	7.33 m/7.32 m	23.3/23.4 CH_3	1.07 d (6.2)/0.91 d (6.7)	13.9/15.6 CH_3	1.15 d (6.8)/ 1.06 d (6.6)
23	126.9/127.1 CH	7.26 m/7.26 m				

[a]For full NMR data, see the Supporting Information. [b]H-18 upfield conformer/H-18 downfield conformer.

dx.doi.org/10.1021/jo502370b | J. Org. Chem. 2015, 80, 304–312

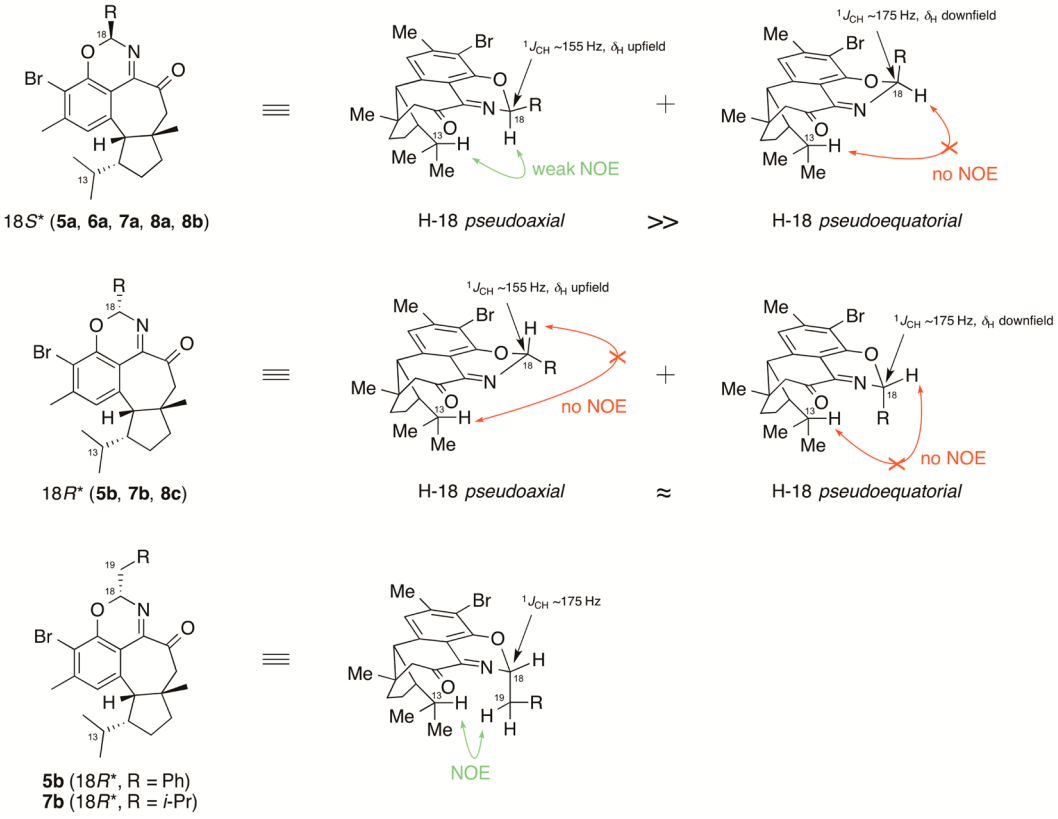

Figure 4. C-18 stereochemical relationships verified by the Perlin effect and NOE correlation data.

compound in this series, 18-*epi*-hamigeran Q (**8c**), showed the same suite of spectroscopic features as compounds **5b** and **7b**. Like its constitutional isomers **8a** and **8b**, the relative configuration about CH-19 in **8c** is also unresolved.

Structural Revision of Hamigeran D. Given the spectroscopic characteristics of compounds **5a**–**8c**, we felt that it was necessary to revisit the reported structure of hamigeran D (**1a**, 18*R*-**1**) and its decomposition product (**2a**, 18*R*-**2**). As drawn in the original articles (as compound **6** in ref 1 and compound **III** in ref 21),[1,22] the relative configuration about C-18 of hamigeran D indicated by the bond-angle diagram is not consistent with our sample, where despite the experimentally identical 1D NMR data, H-13 and H-18 were observed to interact in through-space NMR experiments (1D and 2D NOESY). In addition, the spectroscopic features associated with our reported C-18 epimers (solution conformers with increased $^1J_{CH}$ at CH-18) were not present in our sample. The crystallographic data presented for the reported decomposition product of hamigeran D[22,23] (see the Supporting Information) are consistent with structure **2b** (18*S*-**2**) and in agreement with our findings, suggesting that the original bond-angle diagram was incorrectly drawn. These experimental data imply that the same change is required for the natural product, and as the parent structure in this series of compounds, the configuration of CH-18 in hamigeran D should therefore be changed to structure **1b** (18*S*-**1**).

Biological Activity. Seven of the compounds described in this study were tested for their cytotoxicity against the HL-60 promyelocytic leukemic cell line using an MTT cell proliferation assay, the results of which are summarized in Table 4. Our sample of hamigeran D (**1b**) exhibited a similar response in this assay as that originally reported (P-388, IC_{50} = 8 μM).[1] Of the new compounds that were tested, hamigeran M (**4**) exhibited the highest degree of potency at 6.9 μM. The cytotoxicities displayed by compounds **5a**–**6a** and **7a**–**8a** were similar in magnitude to those for previously reported hamigerans.[2]

Table 4. Nitrogenous Hamigeran IC_{50} Values (HL-60, n = 3 Preparations)

compound	mean IC_{50} ± SEM (μM)
hamigeran D (**1b**)	6.1 ± 0.3
hamigeran M (**4**)	6.9 ± 0.4
hamigeran N (**5a**)	19.5 ± 0.6
18-*epi*-hamigeran N (**5b**)	14.1 ± 0.4
hamigeran O (**6a**)	14.7 ± 0.4
hamigeran P (**7a**)	21.3 ± 0.7
18-*epi*-hamigeran P (**7b**)	11.6 ± 0.2
hamigeran Q (**8a**)	33.3 ± 0.6

Proposed Biogenesis. The biogenetic origin of the nitrogen in the hamigerans described in our study can be ascribed to an amino acid source, rationalized as shown in Scheme 1. The nature of these nitrogenous side chains is consistent with decarboxylated phenylalanine, valine, leucine, and isoleucine. It is therefore entirely reasonable that the additional features of hamigerans D (**1b**) and M (**4**) are derived from decarboxylated alanine and glycine residues, respectively. In the case of **8a**–**c**, the occurrence of three isoleucine-based structures requires that at least one must be derived from *allo*-isoleucine (D- or L-), typical of prokaryotic secondary metabolism.

Hamigeran G (**3**) can be seen as the precursor of the terpenoid skeleton of the nitrogenous compounds, the

dx.doi.org/10.1021/jo502370b | J. Org. Chem. 2015, 80, 304–312

Scheme 1. Proposed Formation of Nitrogenous Hamigerans from Geranyl Geranyl Diphosphate (GGPP)

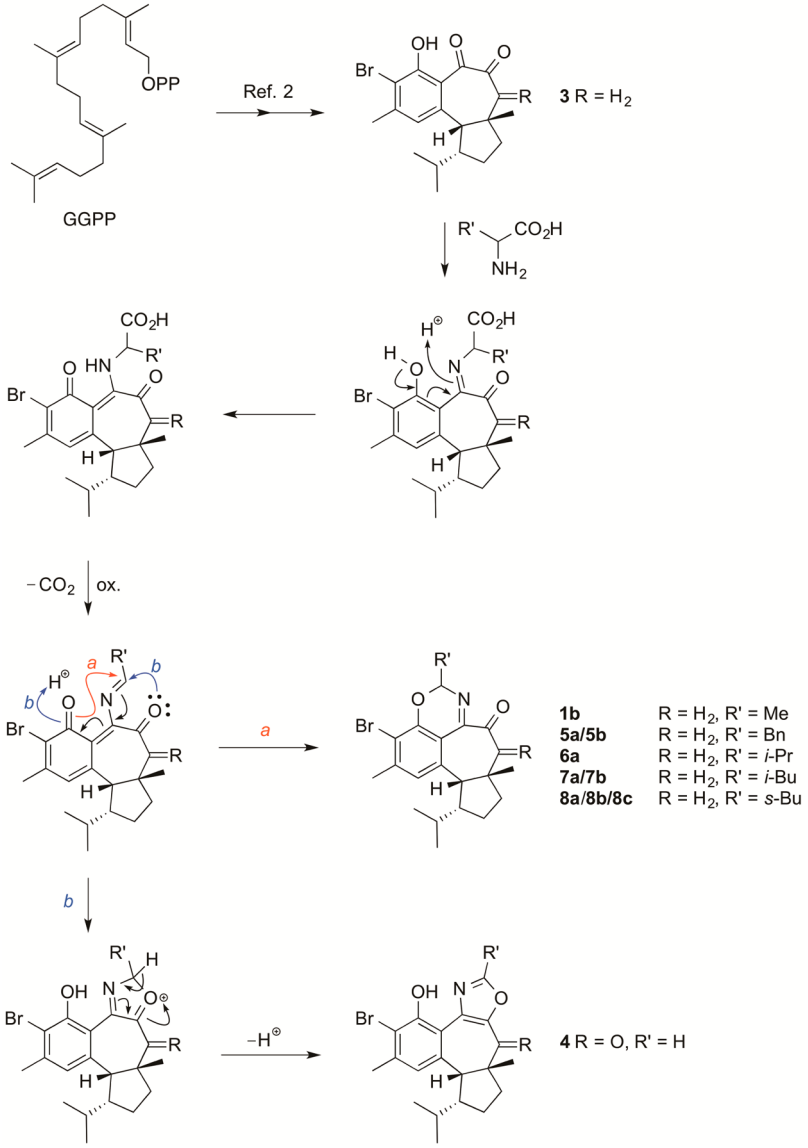

formation of which through the isohamigerane carbon skeleton was proposed in our previous report.[2] Formation of the C-18 aminal requires appropriate functionalization about the α-carbon of the given amino acid, which presumably occurs post-decarboxylation. Attachment of this amino acid by Schiff base chemistry, tautomerisation of the phenol, and subsequent decarboxylative elimination affords a heterodiene, from which a sigmatropic ring closure through pathway *a* (black and red arrow formalism) affords the heterocyclic structure common to compounds **1b**, **5a**–**6a**, and **7a**–**8c**. Alternatively, pathway *b* (black and blue arrow formalism) provides a route to the formation of the oxazole moiety present in hamigeran M (**4**), for which glycine must be considered as the logical amino acid precursor. The occurrence of the C-10 ketone in hamigeran M is unusual, given that all of the other nitrogenous hamigerans possess a methylene unit at this position. Perhaps the presence of this ketone contributes to the formation of the oxazole moiety (pathway *b*) from the proposed glycine adduct through stabilization or extension of conjugation. A recent article highlights the use of Schiff base chemistry toward the preparation of pseudopteroxazole derivatives from the *o*-quinone of the pseudopterosin aglycone.[24] This synthetic method lends credence to the formation of **4** from glycine and alludes to the existence of naturally occurring and synthetically accessible C-18-substituted hamigeran oxazoles.

Reports of nitrogenous terpenes isolated from the marine environment, in which the nitrogen is clearly derived from amino acids, are relatively uncommon. The oxeatamides, a series of nitrogen-containing spongian diterpenes reported by our laboratory, are among the more recent additions.[25] Other reported amino acid/terpene conjugates include but are not limited to the molliorins,[26−29] haumanamide,[30] and the closely related spongolactams.[31] Among the terpenes of marine origin, the diterpene pseudopteroxazole and its congeners[32−34] and the merosesquiterpenoids najikinol,[35] najikinol B,[36] and an unnamed congener[37] appear to be the only compounds that contain an oxazole moiety. It is of particular interest to note that in contrast to hamigeran M (**4**), these compounds exclusively feature benzo-fused oxazoles.

dx.doi.org/10.1021/jo502370b | J. Org. Chem. 2015, 80, 304−312

CONCLUSIONS

The hamigerans possess an unusual array of functionalization for terpenes, including the combination of aromaticity, halogenation, and/or nitrogenous adducts. In this study, the subset of nitrogenous compounds has been extended to 10 structures, bringing the total number of reported natural hamigerans across all structural types to 27. To the best of our knowledge, the isolation of hamigeran M (**4**) represents the first instance of a non-benzo-fused, oxazole-containing terpenoid isolated from the marine environment. Access to variation in the configuration of CH-18 in compounds **5a**−**6a** and **7a**−**8c** has allowed for the reassignment of this position in the archetypal compound hamigeran D, now reported as structure **1b**. The occurrence of constitutional isomers **8a**−**c** indicates the involvement of an *allo*-isoleucine, which is a nonribosomal amino acid normally associated with prokaryotic biosynthesis. The hamigeran terpene core, however, is typical of sponge (eukaryotic) terpene biosynthesis. The combination of these features suggests the possibility of mixed-organism biogenesis.

EXPERIMENTAL SECTION

General Experimental. NMR spectra were acquired on a 600 MHz spectrometer equipped with a triple-resonance HCN cryogenic probe operating at 25 K, with chemical shifts (δ, ppm) referenced to the residual solvent peak.[38] Optical rotations were measured on a polarimeter. High-resolution masses were obtained on a Q-TOF LC−MS equipped with a binary pump and a Q-TOF spectrometer. UV data were measured on a dual-beam spectrophotometer. Semi-preparative and analytical-scale HPLC was performed using a solvent delivery system with 25 mL pump heads. UV/vis detection for HPLC runs was obtained with a photodiode array detector. Solvents used for flash normal- and reversed-phase column chromatography were of HPLC- or analytical-grade quality. All other solvents were purified by distillation before use. Solvent mixtures are reported as % v/v unless otherwise stated.

Animal Material. *Hamigera tarangaensis* was collected by hand using SCUBA from Cavalli Island, New Zealand, in December 2003 and stored at −20 °C until extraction. A voucher sample for this specimen is stored at the School of Chemical and Physical Sciences, Victoria University of Wellington.

Isolation of Compounds. *Hamigeran M.* A frozen sample of *H. tarangaensis* (202 g), collected from Cavalli Island, New Zealand, was extracted with MeOH (2 × 1 L) and fractionated from PSDVB (1 L, pre-equilibrated in MeOH) with 3 L portions of (i) 20% Me_2CO/H_2O (fraction A), (ii) 40% Me_2CO/H_2O (fraction B), (iii) 60% Me_2CO/H_2O (fraction C), (iv) 80% Me_2CO/H_2O (fraction D), and (v) Me_2CO (fraction E). The 80% Me_2CO/H_2O fraction was partitioned on LH-20 using 50% MeOH/CH_2Cl_2 as the running solvent. Three hamigeran-containing fractions (F−H) were identified by TLC and ^{1}H NMR analysis. Fraction H was subjected to semipreparative C18 HPLC (75% MeOH/0.2 M HCOOH(aq)) to obtain 15 fractions (I−W), in which fractions I−N and P−W contained previously described hamigerans.[2] Fraction O (t_R = 32.2 min) was finally purified using analytical C18 HPLC (75% MeCN/0.2 M HCOOH(aq)) to afford hamigeran M (**4**) (t_R = 57.5 min, 1.0 mg).

Hamigerans N−Q, 19-epi-Hamigeran Q, and 18-epi-Hamigerans N, P, and Q. A second sample of *H. tarangaensis* (25 g), collected from Cavalli Island, New Zealand, was extracted with MeOH (2 × 100 mL) and fractionated from PSDVB (30 mL, pre-equilibrated in MeOH) with 100 mL portions of (i) 20% Me_2CO/H_2O (fraction A), (ii) 40% Me_2CO/H_2O (fraction B), (iii) 60% Me_2CO/H_2O (fraction C), (iv) 80% Me_2CO/H_2O (fraction D), and (v) Me_2CO (fraction E). The 80% Me_2CO/H_2O fraction was separated on LH-20 using 50% MeOH/CH_2Cl_2 as the running solvent. Three hamigeran-containing fractions (F−H) were identified by TLC and ^{1}H NMR analysis.

The *n*-hexane-soluble portion of fraction G was applied to DIOL column chromatography, eluting with a stepwise *n*-hexane/CH_2Cl_2 gradient (0−100%) to obtain fractions I−N. The *n*-hexane eluents (I−K) were further purified using analytical (4.6 mm × 250 mm, 1 mL/min) and semipreparative (10 mm × 250 mm, 4 mL/min) octadecyl-derivatized silica (C18) HPLC techniques. Fraction I was applied to semipreparative C18 HPLC (85% MeOH/H_2O), yielding fractions O−S as a mixture of **6a** and **6b** (fraction O; t_R = 26.6 min, 1.1 mg), **6a** (fraction P; t_R = 28.5 min, 2.0 mg), a mixture of **7a** and **8c** (fraction Q; t_R = 33.4 min, 2.9 mg), **8b** (fraction R; t_R = 37.2 min, 0.4 mg), and **8a** (fraction S; t_R = 38.6 min, 1.2 mg). Octyl-derivatized silica (C8) HPLC (90% MeCN/H_2O, 0.7 mL/min) was used to purify fraction Q, giving **7a** (t_R = 12.3 min, 1.6 mg) and **8c** (t_R = 12.8 min, 0.7 mg).

Fraction J was subjected to C18 semipreparative HPLC (80% MeCN/H_2O) to yield compound **1b** (fraction T; t_R = 8.6 min, 1.2 mg), compound **5a** (fraction U; t_R = 13.9 min, 1.7 mg), and a mixture of compounds **7a** and **7b** (fraction V). Fraction V required further purification by C8 analytical HPLC (75% MeCN/H_2O), giving compounds **7b** (t_R = 32.1 min, 1.8 mg) and **7a** (t_R = 33.9 min, 0.8 mg). Compound **5b** was isolated from fraction K using C18 semipreparative HPLC (80% MeCN/H_2O, t_R = 18.7 min) and C18 analytical HPLC (75% MeCN/H_2O, t_R = 33.7 min, 0.8 mg) separation steps, along with hamigeran D (**1b**) (1.0 mg).

Characterization Data. *Hamigeran D (**1b**).* Pale-yellow film; $[\alpha]_D^{23}$ −233 (*c* 0.08, CH_2Cl_2); UV (MeOH) λ_{max}/nm (log ε) 211 (4.50), 324 (3.58); for NMR data, see Table 2 and the Supporting Information; HR-ESI-MS $[M + Na]^+$ observed *m*/*z* 426.1042, calculated 426.1039 for $C_{21}H_{26}NO_2{}^{79}BrNa$, Δ = +0.6 ppm; all other data as previously described.[1]

*Hamigeran M (**4**).* Pale-yellow film; $[\alpha]_D^{23}$ −19 (*c* 0.03, CH_2Cl_2); UV (MeOH) λ_{max}/nm (log ε) 214 (4.31), 342 (3.65); for NMR data, see Table 1; HR-ESI-MS $[M + Na]^+$ observed *m*/*z* 426.0689, calculated 426.0681 for $C_{20}H_{22}NO_3{}^{79}BrNa$, Δ = +2.0 ppm.

*Hamigeran N (**5a**).* Colorless film; $[\alpha]_D^{23}$ −197 (*c* 0.11, CH_2Cl_2); UV (MeOH) λ_{max}/nm (log ε) 211 (4.59), 324 (3.54); for NMR data, see Table 2 and the Supporting Information; HR-ESI-MS $[M + Na]^+$ observed *m*/*z* 502.1358, calculated 502.1352 for $C_{27}H_{30}NO_2{}^{79}BrNa$, Δ = +1.2 ppm.

*18-epi-Hamigeran N (**5b**).* Colorless film; $[\alpha]_D^{23}$ −104 (*c* 0.05, CH_2Cl_2); UV (MeOH) λ_{max}/nm (log ε) 211 nm (4.38), 328 (3.28); for NMR data, see Table 3 and the Supporting Information; HR-ESI-MS $[M + Na]^+$ observed *m*/*z* 502.1356, calculated 502.1352 for $C_{27}H_{30}NO_2{}^{79}BrNa$, Δ = +0.8 ppm.

*Hamigeran O (**6a**).* Colorless film; $[\alpha]_D^{23}$ −245 (*c* 0.07, CH_2Cl_2); UV (MeOH) λ_{max}/nm (log ε) 213 (4.57), 324 (3.55); for NMR data, see Table 2 and the Supporting Information; HR-ESI-MS $[M + Na]^+$ observed *m*/*z* 454.1354, calculated 454.1352 for $C_{23}H_{30}NO_2{}^{79}BrNa$, Δ = +0.4 ppm.

*Hamigeran P (**7a**).* Colorless film; $[\alpha]_D^{23}$ −215 (*c* 0.05, CH_2Cl_2); UV (MeOH) λ_{max}/nm (log ε) 213 (4.51), 326 (3.47); for NMR data, see Table 2 and the Supporting Information; HR-ESI-MS $[M + Na]^+$ observed *m*/*z* 468.1506, calculated 468.1509 for $C_{24}H_{32}NO_2{}^{79}BrNa$, Δ = −0.5 ppm.

*18-epi-Hamigeran P (**7b**).* Colorless film; $[\alpha]_D^{23}$ −140 (*c* 0.12, CH_2Cl_2); UV (MeOH) λ_{max}/nm (log ε) 214 (4.42), 323 (3.38); for NMR data, see Table 3 and the Supporting Information; HR-ESI-MS $[M + Na]^+$ observed *m*/*z* 468.1513, calculated 468.1509 for $C_{24}H_{32}NO_2{}^{79}BrNa$, Δ = +1.0 ppm.

*Hamigeran Q (**8a**).* Colorless film; $[\alpha]_D^{23}$ −235 (*c* 0.06, CH_2Cl_2); UV (MeOH) λ_{max}/nm (log ε) 213 (4.47), 328 (3.43); for NMR data, see Table 2 and the Supporting Information; HR-ESI-MS $[M + Na]^+$ observed *m*/*z* 468.1510, calculated 468.1509 for $C_{24}H_{32}NO_2{}^{79}BrNa$, Δ = +0.3 ppm.

*19-epi-Hamigeran Q (**8b**).* Colorless film; $[\alpha]_D^{25}$ −207 (*c* 0.03, CH_2Cl_2); UV (MeOH) λ_{max}/nm (log ε) 214 (4.41), 307 (3.33); for NMR data, see Table 2 and the Supporting Information; HR-ESI-MS $[M + H]^+$ observed *m*/*z* 446.1694, calculated 446.1689 for $C_{24}H_{33}NO_2{}^{79}Br$, Δ = −1.1 ppm.

*18-epi-Hamigeran Q (**8c**).* Colorless film; $[\alpha]_D^{25}$ −72 (*c* 0.05, CH_2Cl_2); UV (MeOH) λ_{max}/nm (log ε) 214 (4.41), 307 (3.39); for

dx.doi.org/10.1021/jo502370b | J. Org. Chem. 2015, 80, 304−312

NMR data, see Table 3 and the Supporting Information; HR-ESI-MS $[M + H]^+$ observed m/z 446.1693, calculated 446.1689 for $C_{24}H_{33}NO_2{}^{79}Br$, Δ = +1.0 ppm.

Cell Proliferation Assays. 3-(4,5-Dimethylthiazol-2-yl)-2,5-diphenyltetrazolium bromide (MTT) cell proliferation assays using the HL-60 promyelocytic leukemic cell line were performed as previously described.[39]

■ ASSOCIATED CONTENT

Supporting Information

Isolation schemes, full NMR data tables, and 1D and 2D NMR spectra for compounds **4**, **5a**−**6a**, and **7a**−**8c**. This material is available free of charge via the Internet at http://pubs.acs.org.

■ AUTHOR INFORMATION

Corresponding Author

*E-mail: peter.northcote@vuw.ac.nz. Tel: +64-4-463-5960.

Notes

The authors declare no competing financial interest.

■ ACKNOWLEDGMENTS

J.D.D. was a Visiting Scholar at Victoria University of Wellington. Funding from Victoria University of Wellington (A.J.S.), the Wellington Medical Research Foundation (J.H.M.), the New Zealand Cancer Society (J.J.F., J.H.M.), and the University of Richmond School of Arts and Sciences (J.D.D.) is acknowledged. Ian Vorster (Victoria University of Wellington) and Yinrong Lu (Callaghan Innovation) are thanked for performing MS measurements.

■ REFERENCES

(1) Wellington, K. D.; Cambie, R. C.; Rutledge, P. S.; Bergquist, P. R. *J. Nat. Prod.* **2000**, *63*, 79−85.
(2) Singh, A. J.; Dattelbaum, J. D.; Field, J. J.; Woolly, E. F.; Smart, Z.; Barber, J. M.; Heathcott, R.; Miller, J. H.; Northcote, P. T. *Org. Biomol. Chem.* **2013**, *11*, 8041−8051.
(3) Nicolaou, K. C.; Gray, D.; Tae, J. *Angew. Chem., Int. Ed.* **2001**, *40*, 3675−3678.
(4) Nicolaou, K. C.; Gray, D.; Tae, J. *Angew. Chem., Int. Ed.* **2001**, *40*, 3679−3683.
(5) Clive, D. L. J.; Wang, J. *Angew. Chem., Int. Ed.* **2003**, *42*, 3406−3409.
(6) Clive, D. L. J.; Wang, J. *Tetrahedron Lett.* **2003**, *44*, 7731−7733.
(7) Mehta, G.; Shinde, H. M. *Tetrahedron Lett.* **2003**, *44*, 7049−7053.
(8) Clive, D. L. J.; Wang, J. *J. Org. Chem.* **2004**, *69*, 2773−2784.
(9) Nicolaou, K. C.; Gray, D. L. F.; Tae, J. *J. Am. Chem. Soc.* **2004**, *126*, 613−627.
(10) Trost, B. M.; Pissot-Soldermann, C.; Chen, I.; Schroeder, G. M. *J. Am. Chem. Soc.* **2004**, *126*, 4480−4481.
(11) Clive, D. L. J.; Wang, J. *Org. Prep. Proced. Int.* **2005**, *37*, 1−35.
(12) Taber, D. F.; Tian, W. *J. Org. Chem.* **2008**, *73*, 7560−7564.
(13) Lau, S. Y. W. *Org. Lett.* **2011**, *13*, 347−349.
(14) Jiang, B.; Li, M.-m.; Xing, P.; Huang, Z.-g. *Org. Lett.* **2013**, *15*, 871−873.
(15) Julianti, E.; Oh, H.; Lee, H.-S.; Oh, D.-C.; Oh, K.-B.; Shin, J. *Tetrahedron Lett.* **2012**, *53*, 2885−2886.
(16) Banert, K. *Tetrahedron Lett.* **2012**, *53*, 6443−6445.
(17) Januar, L. A.; Molinski, T. F. *Org. Lett.* **2013**, *15*, 2370−2373.
(18) Sisko, J.; Kassick, A. J.; Mellinger, M.; Filan, J. J.; Allen, A.; Olsen, M. A. *J. Org. Chem.* **2000**, *65*, 1516−1524.
(19) Perlin, A. S.; Casu, B. *Tetrahedron Lett.* **1969**, *10*, 2921−2924.
(20) Wolfe, S.; Pinto, B. M.; Varma, V.; Leung, R. Y. N. *Can. J. Chem.* **1990**, *68*, 1051−1062.
(21) Matsumori, N.; Kaneno, D.; Murata, M.; Nakamura, H.; Tachibana, K. *J. Org. Chem.* **1999**, *64*, 866−876.
(22) Cambie, R. C.; Rickard, C. E. F.; Rutledge, P. S.; Wellington, K. D. *Acta Crystallogr., Sect. C* **2001**, *57*, 958−960.
(23) Cambridge Crystallographic Data Centre; http://www.ccdc.cam.ac.uk/ (accessed May 20, 2014).
(24) McCulloch, M. W. B.; Berrue, F.; Haltli, B.; Kerr, R. G. *J. Nat. Prod.* **2011**, *74*, 2250−2256.
(25) Wojnar, J. M.; Dowle, K. O.; Northcote, P. T. *J. Nat. Prod.* **2014**, *77*, 2288−2295.
(26) Cafieri, F.; de Napoli, L.; Fattorusso, E.; Santacroce, C.; Sica, D. *Tetrahedron Lett.* **1977**, *18*, 477−480.
(27) Cafieri, F.; de Napoli, L.; Fattorusso, E.; Santacroce, C. *Experientia* **1977**, *33*, 994−995.
(28) Cafieri, F.; de Napoli, L.; Iengo, A.; Santacroce, C. *Experientia* **1978**, *34*, 300−301.
(29) Cafieri, F.; de Napoli, L.; Iengo, A.; Santacroce, C. *Experientia* **1979**, *35*, 157−158.
(30) Pham, A. T.; Carney, J. R.; Yoshida, W. Y.; Scheuer, P. J. *Tetrahedron Lett.* **1992**, *33*, 1147−1148.
(31) Mori, D.; Kimura, Y.; Kitamura, S.; Sakagami, Y.; Yoshioka, Y.; Shintani, T.; Okamoto, T.; Ojika, M. *J. Org. Chem.* **2007**, *72*, 7190−7198.
(32) Rodríguez, A. D.; Ramírez, C.; Rodríguez, I. I.; González, E. *Org. Lett.* **1999**, *1*, 527−530.
(33) Rodríguez, I. I.; Rodríguez, A. D. *J. Nat. Prod.* **2003**, *66*, 855−857.
(34) Rodríguez, I. I.; Rodríguez, A. D.; Wang, Y.; Franzblau, S. G. *Tetrahedron Lett.* **2006**, *47*, 3229−3232.
(35) Kobayashi, J. i.; Madono, T.; Shigemori, H. *Tetrahedron Lett.* **1995**, *36*, 5589−5590.
(36) Ovenden, S. P. B.; Nielson, J. L.; Liptrot, C. H.; Willis, R. H.; Tapiolas, D. M.; Wright, A. D.; Motti, C. A. *J. Nat. Prod.* **2011**, *74*, 65−68.
(37) Stewart, M.; Fell, P. M.; Blunt, J. W.; Munro, M. H. G. *Aust. J. Chem.* **1997**, *50*, 341−348.
(38) Gottlieb, H. E.; Kotlyar, V.; Nudelman, A. *J. Org. Chem.* **1997**, *62*, 7512−7515.
(39) Hood, K. A.; West, L. M.; Northcote, P. T.; Berridge, M. V.; Miller, J. H. *Apoptosis* **2001**, *6*, 207−219.